*promoting access to White Rose research papers*

## Universities of Leeds, Sheffield and York
## http://eprints.whiterose.ac.uk/

White Rose Research Online URL for this paper:
http://eprints.whiterose.ac.uk/78883

**Published paper**

Squire, J, Maddrell, E.R, Hyatt, N.C and Stennett, M.C (2014) Influence of Lubricants and Attrition Milling Parameters on the Quality of Zirconolite Ceramics, Consolidated by Hot Isostatic Pressing, for Immobilization of Plutonium. International Journal of Applied Ceramic Technology. Doi: 10.1111/ijac.12239

*White Rose Research Online*
*eprints@whiterose.ac.uk*

# Influence of Lubricants and Attrition Milling Parameters on the Quality of Zirconolite Ceramics, Consolidated by Hot Isostatic Pressing, for Immobilization of Plutonium

**Jonathan Squire**

*The National Nuclear Laboratory, Sellafield, Seascale, Cumbria, CA20 1PG, U.K.*

*Department of Materials Science and Engineering, The University of Sheffield, Mappin Street, Sheffield, S1 3JD, U.K.*

**Ewan R. Maddrell**

*The National Nuclear Laboratory, Sellafield, Seascale, Cumbria, CA20 1PG, U.K.*

**Neil C. Hyatt\* and Martin C. Stennett**

*Department of Materials Science and Engineering, The University of Sheffield, Mappin Street, Sheffield, S1 3JD, U.K.*

The effect of attrition milling on the processing of precursor oxides was investigated, with reference to the fabrication of titanate ceramics for the immobilization of plutonium and actinides, consolidated by hot isostatic pressing. Difficulties encountered during the lubricant removal step masked any correlation between the milling conditions and the final product. Four lubricants were investigated zinc stearate, Ceridust™, polyethylene glycol and oleic acid. The precursor blends were added to these lubricants to ensure the powders remained free flowing while dry milling in an attrition mill. All except Ceridust™ allowed the milled powders to be freely discharged. Examination of the products showed that each sample was highly porous and all were below the target minimum of 92 % of theoretical density. XRD and SEM analysis showed the production of a multiphase ceramic (zirconolite, perovskite, ilmenite) rather than the single target phase zirconolite. The impact of incomplete lubricant burn out on the oxidation states of Ce and Fe was investigated by XANES and Mössbauer spectroscopy, respectively. Suggested modifications to the HIP processing line, including the addition of an *in situ* sintered metal filter, the use of fumed metal oxides and the introduction of electrical conductivity in the precursors, are presented.

The United Kingdom holds a considerable stockpile of separated plutonium from the civil fuel cycle, estimated to amount to 104 tHM[1] of UK material and an additional 34 tHM of foreign-owned material at the end of projected reprocessing operations (tHM, metric tons heavy metal). This material was produced as a consequence of the requirement to reprocess fuel from the United Kingdom's first generation of power reactors, the Magnox fleet, and continued operations in the THORP reprocessing plant. It was originally intended that plutonium would be recycled as a mixed oxide fuel (MOX, $(U, Pu)O_2$) in a fast reactor program, which was subsequently canceled in 1994. Consequently, the absence of suitable operational reactors to consume plutonium has allowed this fissile material to accumulate, attracting international concern.[2] Following public consultation,

Government set out its position regarding the long-term management of civil plutonium stocks in December 2011, stating that: "the preferred policy for managing the vast majority of UK civil separated plutonium is reuse and it therefore should be converted to MOX fuel for use in civil nuclear reactors. Any remaining plutonium whose condition is such that it cannot be converted into MOX will be immobilized and treated as waste for disposal".[3]

The Nuclear Decommissioning Authority, responsible for implementing UK Government policy, identified four potential immobilization options for separated plutonium: cements and polymers, glasses, ceramics, and so-called "disposal" or "low specification" MOX.[4] It is considered that encapsulation of plutonium in a cementitious wasteform would necessitate very low waste loading, leading to around 200,000 tons of cemented product.[5] This low waste loading requirement is a result of criticality concerns of encapsulating a fissile material

in a highly moderated environment.[6] Consequently, several encapsulation plants and many thousands of containers would be required to dispose of the entire stockpile in a timely fashion. The consideration of cement encapsulation of plutonium as a potential wasteform is based, primarily, on considerable operating experience in the cementation of intermediate level wastes.[7] The United Kingdom also has considerable experience in the vitrification of high-level nuclear wastes arising from spent nuclear fuel reprocessing and vitrification of plutonium in durable glass wasteforms has been widely considered.[8–12] However, vitrification is complicated by the low solubility of plutonium (leading to low waste loadings) generally achieved using standard borosilicate glasses (4–5 wt%), high melting temperatures required, and accountancy concerns associated with a continuous melting process.[13] The fabrication of "disposal MOX" assumes the same manufacturing process for MOX fuel, but with less stringent product dimensional controls. Although this is a mature technology in principle, the fabrication of large monolithic ceramics is clearly preferred to the production of many small bodies of fuel pellet dimensions. Furthermore, this approach does not introduce any significant barrier to address proliferation concerns. The ceramic immobilization option considered by NDA does not define a specific product; however, consolidation by Hot Isostatic Pressing is highlighted as a favored technology. The advantages of ceramic wasteforms have been widely documented[14–19] and include high waste loading of actinide (surrogates), excellent aqueous durability, tolerance to self-induced radiation damage (verified by natural analogs),[20] and excellent proliferation resistance. The generic design and processing considerations for such a ceramic wasteform, in the UK context, have been recently documented.[21] HIP technology operates by the application of high pressures and temperatures to oxide powders contained within a sealed HIP can. This approach has many advantages: it generates minimal secondary wastes, it is insensitive to wasteform physical properties, it is a batch process, there are no volatile losses during consolidation, and it is largely independent of processing scale. Although there are no current examples of a full-scale active ceramic waste immobilization plant, hot isostatic pressing technology has been demonstrated at full scale with inactive radioactive waste simulants and is widely used in the fabrication of high-performance ceramics.[22,23]

Building on the multiphase SYNROC titanate ceramic developed by ANSTO, in which the many components of a high-level waste stream can be co-immobilized, tailored ceramic wasteforms for separated plutonium have developed. For example, in SYNROC-C

(an assemblage of hollandite, perovskite, zirconolite, and rutile) actinides typically partition into the zirconolite phase,[24] which can therefore be targeted as a single plutonium host phase ceramic wasteform. The aim of this research was to investigate the influence of lubricants on the powder processing of zirconolite precursor materials, prior to consolidation by Hot Isostatic Pressing (HIP).

Zirconolite, ideally $CaZrTi_2O_7$, may be considered a monoclinic derivative of the cubic pyrochlore structure. Actinides and lanthanides can be substituted onto both the Ca and Zr sites with suitable charge balancing on the Ti-site. For example, $Pu^{4+}/Ce^{4+}$ can be substituted onto the $Ca^{2+}$ site by balancing the charge with $Fe^{3+}$ on the $Ti^{4+}$ site to give $Ca_{1-x}(Pu,Ce)_xZrTi_{2-2x}Fe_{2x}O_7$; the Pu solid solution of this type was recently documented by Gilbert et al.[25] Natural zirconolites show many different combinations of element substitutions, demonstrating excellent chemical flexibility, and resistance to aqueous dissolution is admirable.[26] Zirconolite also exhibits exceptional corrosion resistance up to 250°C in various acidic and basic solutions, which is important for demonstrating resistance to proliferation.[27] Operating regimes for consolidation of zirconolite ceramics by HIPing typically involve temperatures in the region of 1300°C (generally limited by the HIP can material) and an applied pressure of 100 MPa Ar.[28]

A typical immobilization process would combine homogenization, size reduction, and consolidation into a series of batch processes. Size reduction may be necessary to allow full phase development to occur at lower operating temperatures and dwell times, important for the bulk manufacture of wasteforms. Homogenization ensures that all components of the feed are uniformly mixed and there are no areas of increased localized waste concentration. The general design philosophy is to minimize the number of processing steps and, accordingly, these two steps can be combined in an attrition mill.

Attrition mills, generically known as stirred ball mills, are often used in the manufacture of ceramics. The mills consist of a static outer milling pot containing approximately two thirds of the empty volume of milling media. The media may be zirconia, stainless steel or alumina in ball or platelet form. A central shaft containing short horizontal bars agitates the media. Attrition mills have previously been incorporated as a key plant item in the Sellafield MOX Plant.[29] To satisfy the general design principle of minimizing secondary effluents, the mill must be operated in the dry mode, that is, without carrier fluid. Ensuring the powders remain free flowing during milling can be problematic in this operating mode. If the powders are allowed to settle on the base of the mill they will compact into an immovable

agglomerated mass that prevents mill discharge. Lubricants, typically hydrocarbon waxes, must be added to minimize such an occurrence. However, difficulties can arise when removing lubricants postmilling. Full and complete removal is essential to ensure a high product quality and not to undermine the scientific basis for wasteform performance. A full-scale process would discharge powders from the mill directly into a HIP can and the lubricant would be removed, through heating under vacuum, directly from the HIP can *in situ*.

The focus of this work is the application of an attrition mill to the development of candidate plutonium wasteforms consolidated by HIP with particular focus on the ability of different lubricants to ensure powders are kept free flowing throughout milling.

## Material and Methods

Zirconolite was chosen as the target ceramic wasteform for this work. We elected to substitute 0.25 formula units of Ce, targeted as $Ce^{4+}$, on the Ca-site, with co-substitution of $Fe^{2/3+}$ (supplied as $Fe_3O_4$) for charge balancing *via* substitution on the Ti-site. $Ce^{4+}$ is used as a $Pu^{4+}$ [30,31] surrogate due to their similar ionic radii, 1.11 and 1.10 Å, respectively, in eightfold coordination. As this study was concerned with demonstration of the proposed approach, $CeO_2$ was used as a surrogate for $PuO_2$, on grounds of safety, cost, and expediency. We acknowledge that such a surrogate cannot fully reproduce the physical and chemical behavior of another element. However, Ce is among the most useful and representative inactive Pu surrogates, albeit with limitations including different redox potentials.[30,31] For a comprehensive review of the suitability and shortcomings of using Ce as a Pu surrogate, in the context of glass and ceramic wasteforms, we refer the reader to the study of Bingham *et al.*[30]

The mixed valency of Fe was also expected to aid scanning electron microscope (SEM) imaging by producing an electrically conductive sample. Thus, the target stoichiometry was $Ca_{0.75}Ce_{0.25}ZrTi_{1.625}Fe_{0.375}O_7$.

The raw powders were either as purchased metal oxides ($Fe_3O_4$, $CeO_2$, $ZrO_2$) all supplied by Alfa Aesar or from a premixed batch which was being used for another aspect of our wasteform development work looking at Ti-pyrochlore wasteforms. The batch was, by mass fraction, 21.3 % CaO, 8.7 % $ZrO_2$ and 70.0 % $TiO_2$. This material had been calcined at 1200°C for 10 h to guard against carbonation and stabilize the CaO as perovskite, $CaTiO_3$. An additional 1 wt% of $ZrO_2$ was included which, combined with a small excess of $TiO_2$

in the batch precursor, provides a buffer against the potential formation of deleterious secondary phases. The production of the precursor in a nonactive environment is representative of the intended full-scale process.

Based on previous experience, precursors were mixed in a Turbula Mixer with either 1.5 or 1.0 wt% of lubricant. The four lubricants chosen were zinc stearate, $[CH_3(CH_2)_{16}COO]_2Zn$; Ceridust™ 3620 (Clariant, Muttenz, Switzerland) (a polyethylene wax, $H[CH_2 CH_2]_nH$); polyethylene glycol, $H[OCH_2CH_2]_{~6000}OH$; and oleic acid, $CH_3(CH_2)_7CH= CH(CH_2)_7COOH$. All except oleic acid were supplied as powders.

The attrition mill (Union Process 1SD), pot size 5.6 liters (1.5 US gal), was operated in dry mode. The mill was filled with 16.00 kg of 3/8" Stainless Steel ball bearings (based on the recommendation of the manufacturer). Batches of 800 g (approximately 1 L) of the metal oxide precursors were added to the mill while operating at a tip speed of 1.73 m/s (200 rpm). The mill was quickly brought to the desired speed of 2.16 or 4.32 m/s (250 or 500 rpm) and run for either 30 or 60 min. The mill was discharged while operating at the same speed as when charging. The particle size distribution of the milled powders was typically characterized by $d_{50} \approx 2.5$ µm.

The milled powders were packed into stainless steel HIP cans 60 mm tall by 35 mm outside diameter. Each can was filled with loose material, which was compacted uniaxially by approximately 30 MPa of pressure. The cans were then filled with loose powders again and the process repeated until they were full, typically containing 160–170 g of compressed powders. Lids, with 3 mm inside diameter evacuation tubes, were autogenously welded to the cans. The sealed cans were attached to a vacuum line and heated to 600°C for four hours with the intention of fully removing the lubricant. The bake out temperature was higher than the highest boiling point (260–450°C) of the lubricants. After bake out, the can stems were crimped, cut and welded closed.

The cans were consolidated by HIP at 1320°C and 100 MPa with a 2 h dwell. Heating rates were typically ~8°C per min below 1100°C and <5°C per min otherwise. Pressure was increased steadily with temperature and was kept constant throughout the hold.

A core of the consolidated material was removed from the cans for examination. A section was hot mounted with conductive resin and ground with successively finer grit papers (300, 500, 800) before being polished with 5 and 1 µm diamond suspensions to obtain an optical finish. SEM images were obtained using a JEOL JSM-5600 operating in the back-scattered mode with 15 kV accelerating voltage, spot size of 35

and a working distance of 15 mm. Two images were acquired of the same area: one at 200x magnification and one at 1500×. Energy Dispersive X-ray (Princeton Gamma Technologies with a PRISM Si(Li) digital detector), coupled to the SEM, was used for elemental mapping. Another aliquot was ground into a fine powder and X-ray diffraction data were obtained (Inel Equinox1000) with Co Kα radiation and a resolution of 0.1°. Due to significant Ti fluorescence, it was necessary to smooth the data with a 5-point moving average. Sample densities were measured using the Archimedes method with water as the immersion fluid.

Ce $L_3$ edge X-ray Absorption Spectroscopy (XAS) data were collected from the suite of $Ca_{0.75}Ce_{0.25}Zr$-$Ti_{1.625}Fe_{0.375}O_7$ samples consolidated by HIP. For comparative purposes, data were also collected from a single phase sample of $Ca_{0.75}Ce_{0.25}ZrTi_{1.625}Fe_{0.375}O_7$ prepared by cold uniaxial pressing (CUP) and sintering in air. In addition, $CeO_2$ and $CePO_4$ (with the monazite structure) were also measured as standards for $Ce^{4+}$ and $Ce^{3+}$ XANES, respectively. All data were collected on beamline X23A2 of the National Synchrotron Light Source (NSLS), Brookhaven National Laboratory (BNL), USA. Data were acquired in transmission mode using finely ground specimens dispersed in polyethylene glycol (PEG) to achieve a thickness of one absorption length. Data reduction and analysis was performed using the Athena program.[32]

[57]Fe Mössbauer spectroscopy was carried out at room temperature using a Wissel spectrometer at The University of Sheffield. Experiments were performed in transmission mode using a 50 Ci [57]Co source embedded in a Rh matrix, calibrated relative to α-Fe. Spectra were measured using a constant acceleration waveform at a velocity range of ±6 mm/s. Spectral deconvolution was performed using the commercially available software RECOIL[33] by assigning Lorentzian doublets to represent the different Fe oxidation states and coordination environments in the samples.

## Results

Lubricant performance during milling was judged on the ability of the additive to prevent the powder from compaction (i.e., caking) during the milling operation. For the current purpose, a compaction was considered to be two or more layers of milling balls tightly packed with powder. To clear a compaction, the mill must be fully disassembled and the balls and powders removed by hand, an operation not amenable to a glove box environment. Ceridust™ was the only lubricant that failed to

prevent the compaction of powders in the mill. An approximate measurement of discharge rate was used to rank the other three lubricants; the discharges were timed until approximately 99%, by mass of the milled powders had been collected in a receiving jar. Oleic acid typically allowed the milled powders to be discharged within 2 min, while polyethylene glycol and zinc stearate lubricated powders took between 4 and 10 min to achieve discharge, respectively.

Complete removal of the lubricant during the bake out step would result in a theoretical weight loss of ~1.5 %. However, the actual weight loss was determined to be between 1.0–11.3 % over the range of samples investigated, with no obvious correlation between the type of lubricant and weight loss achieved, see Table 1. During bake out of the HIP cans, an oil like substance was observed when cans were disconnected from the bake out system, which was able to drip back down into the HIP can, indicating that some organic material may remain in the HIP can. Moreover, when the bake out system was disassembled, powder was found in the pipework which could only have come from HIP cans being baked out. It was therefore concluded that weight loss during bake out included a component due to powder material from the HIP can (into the vacuum system) as well as volatiles intended to be removed by the bake out process. The removal of any powder material would not be acceptable in an active operating environment, but can be prevented by using an *in situ* filter in the HIP

**Table 1.  Comparison of Expected Mass Loss After Lubricant Removal Step and Actual Mass Loss**

| Tip Speed (m/s) | Duration (minutes) | Lubricant | Lubricant Addition (%) | Mass Loss (%) |
|---|---|---|---|---|
| 2.16 | 30 | Zinc stearate | 1.5 | 1.7 |
| 2.16 | 60 | Zinc stearate | 1.5 | 1.5 |
| 4.32 | 30 | Zinc stearate | 1.5 | 1.5 |
| 2.16 | 30 | Ceridust™ | 1.5 | 1.5 |
| 2.16 | 60 | Ceridust™ | 1.5 | 1.7 |
| 4.32 | 30 | Ceridust™ | 1.5 | 1.6 |
| 2.16 | 30 | Polyethylene glycol | 1.5 | 3.8 |
| 2.16 | 60 | Polyethylene glycol | 1.5 | 11.2 |
| 4.32 | 30 | Polyethylene glycol | 1.5 | 1.4 |
| 2.16 | 30 | Oleic acid | 1.0 | 1.3 |
| 2.16 | 60 | Oleic acid | 1.0 | 1.1 |
| 4.32 | 30 | Oleic acid | 1.0 | 1.0 |

can design. Further evidence for powder removal was given by the HIP can with the greatest mass loss after bake out in that a large deformation underneath the bake out tube was found after consolidation. This is a result of the HIP can lid being pressed into the void created by the removal of powder.

To determine the density of the samples, a core of material was taken from the consolidated product. During this process, the cut surfaces of the sample produced a hissing sound that was indicative of the release of gas. Many small bubbles forming on the surface of the sample were also observed, accompanied by a smell similar to burnt oil. Even a few minutes after cutting, this sound continued implying the release of pressurized gas from the ceramic matrix. This was a further indication that organic material had persisted in the HIP can through the bake out cycle, and had reacted with the ceramic powders at the HIP temperature. This gas was only released when a suitable pathway for discharge became available. Attempts to quantify the mass of entrained gases, by heating the ceramic product at 2°C per min to 1100°C with an 8 hour dwell, resulted in the ceramic bodies exploding. The explosion indicates an increase in internal pressure within the ceramic, again consistent with the fact that gases form from lubricant residues within the product during the HIP cycle.

The measured densities of the ceramic bodies produced are reported in Table 2 (in order of increasing density). The samples have a range of densities between 79.5% and 89.2% of theoretical density; the estimated errors are $\pm 0.01$ g/cm$^3$ or $\pm 0.2\%$ of theoretical. The theoretical density was calculated as 4.78 g/cm$^3$, based on the published unit cell volume of the zirconolite structure and nominal composition. Shaw[34] determined the critical porosity, the point between closed (i.e., isolated) and open (i.e., interconnected) porosity, to be 92% in plutonium ceramic wasteforms and this was set as the target product density. Elimination of open porosity is desirable to minimize product surface area and with it the corresponding reduction in leach rates. None of the samples prepared in this study were found to exhibit ceramic density above this 92% threshold and there did not appear to be any clear correlation between the speed or duration of milling, choice of lubricant and the final density. An equivalent milled sample, from which the lubricant had been baked out under air in an open furnace HIPped to 97% of the theoretical density.

Figure 1 shows the XRD patterns from samples prepared by hot isostatic pressing of powders prepared by attrition milling at 4.32 m/s for 30 min with various lubricants. As expected, the formation of zirconolite as the major phase is confirmed, for which the correspond-

**Table 2. Density of Samples Ordered by Increasing Theoretical Density**

| Tip Speed (m/s) | Duration (minutes) | Lubricant | Density (g/cm$^3$) | % Theoretical |
|---|---|---|---|---|
| 2.16 | 30 | Ceridust™ | 3.80 | 79.5% |
| 2.16 | 60 | Polyethylene glycol | 3.90 | 81.5% |
| 4.32 | 30 | Oleic acid | 3.98 | 83.2% |
| 2.16 | 30 | Polyethylene glycol | 4.06 | 84.9% |
| 2.16 | 60 | Oleic acid | 4.06 | 84.9% |
| 4.32 | 30 | Polyethylene glycol | 4.06 | 84.9% |
| 2.16 | 30 | Zinc stearate | 4.07 | 85.2% |
| 4.32 | 30 | Ceridust™ | 4.10 | 85.8% |
| 2.16 | 60 | Ceridust™ | 4.16 | 87.0% |
| 2.16 | 60 | Zinc stearate | 4.18 | 87.5% |
| 2.16 | 30 | Oleic acid | 4.26 | 89.1% |
| 4.32 | 30 | Zinc stearate | 4.26 | 89.2% |
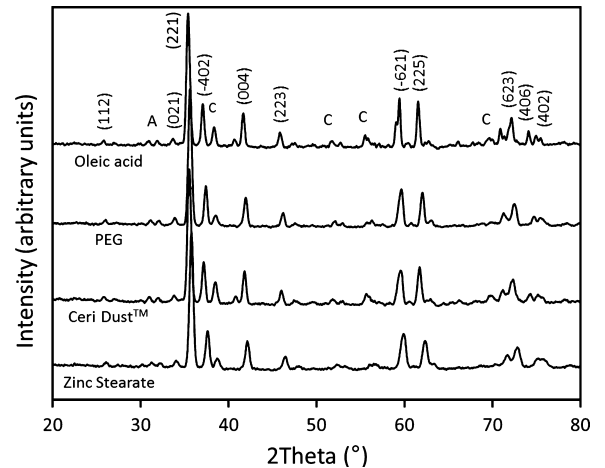


Fig. 1.  XRD patterns from samples prepared by hot isostatic pressing of powders prepared by attrition milling at 4.32 m/s for 30 minutes with various lubricants. From bottom to top, samples were prepared with lubricants of zinc stearate, Ceridust™, polyethylene glycol, oleic acid. Data were smoothed with a moving 5-point average. Miller indices are given for most intense peaks of the zirconolite phase. Other reflections highlighted correspond to, (A) ilmenite (possibly in solid solution with hematite), (C) perovskite phase.

ing major reflections in Fig. 1 are highlighted by the appropriate Miller indices. However, there are also reflections associated with an ilmenite (possibly in solid solution with hematite) and perovskite phase. These

products are clearly not single phase and this could be a concern for a final wasteform if a proportion of actinide inventory is not partitioned into the target zirconolite phase. Interestingly, the four different samples show different proportions of perovskite and zirconolite phases, evaluated on the relative intensity of associated reflections in the XRD patterns. When considering that the same starting materials and milling conditions had been used, it was expected that the samples would show similar diffraction patterns. It can be inferred, therefore, that the choice of lubricant can go on to affect the phase assemblage of the ceramic product, although the mechanism behind this is not yet clear.

Figure 2 shows SEM images of samples prepared by hot isostatic pressing of powders prepared by attrition milling at 4.32 m/s for 30 min with various lubricants. All samples have a large number of pores and this is reflected in the low percentage theoretical densities recorded. The size and distribution of grains and pores appears to be similar throughout the samples. Comparing the effect of lubricant, we do not find any clear difference between the microstructures observed, although, there is a marked increase in the size and number of pores in the lower density products, as expected. All samples are broadly similar, with each image showing a host matrix of zirconolite ($(Ca,Ce)Zr(Ti,Fe)_2O_7$, labeled B) interspersed with dark colored grains with a lower average atomic number. Within many of the dark grains, a distinct core is apparent: EDX analysis of the core region revealed a composition consistent with perovskite (nominally $CaTiO_3$, labeled C), whereas the composition of the outer rim was consistent with a Ce and Fe substituted perovskite (i.e., $(Ca,Ce)(Ti,Fe)O_3$, labeled D). There are also a number of Fe rich grains, identified as ilmenite (prototypically $FeTiO_3$, possibly in solid solution with $Fe_2O_3$, labeled A), as shown in Fig. 3 (and Table 3). These observations are consistent with XRD data.

An example elemental map of a consolidated sample (prepared from powders milled at 4.32 m/s for 30 min with polyethylene glycol as the lubricant) is given in Fig. 4. Ti has a homogeneous distribution throughout the product. Zr is equally distributed throughout the bulk with no Zr observed within the perovskite grains. Ca also tends to be well distributed in the primary zirconolite phase but with localized concentrations in the perovskite phases. Fe is most concentrated in the ilmenite phase; however, the zirconolite phase still contains Fe as the designated charge compensator. Ce does not exhibit any localized concentrations and this is considered an encouraging observation because agglomerations of Pu within the wasteform would be undesirable. The

tendency for $Ce^{4+}$ to reduce to $Ce^{3+}$ will increase the amount of perovskite (compared to the real scenario in which $Pu^{4+}$ is more stable), as trivalent lanthanides are known to stabilize cation deficient perovskite solid solutions over a wide composition range.[35] In agreement with this hypothesis, Gilbert et al.[25] studied the corresponding $Ca_{1-x}(Pu,Ce)_xZrTi_{2-2x}Fe_{2x}O_7$ solid solution, fabricated by the CUP route, and reported single phase zirconolite for the relevant composition with x ≈ 0.25.

The grain map and the SEM both show that the product is not homogenous with a large number of perovskite grains interspersed in the zirconolite matrix. Perovskite has been shown to be thermodynamically unstable in repository environments[26] and is also significantly less durable than the intended host phase zirconolite. The EDX analysis shows a proportion of the Ce has partitioned into these grains and this could be a concern for the wasteform performance. The fraction of Ce inventory in zirconolite and perovskite has not been measured. It is believed that the perovskite inclusions were formed during the precursor heat treatment to stabilize CaO as $CaTiO_3$, and that these were robust enough to persist through attrition milling. The amount of $Ce^{3+}$ partitioning into perovskite has probably been exacerbated by the provenance of the perovskite. That is, the perovskite is present because the inclusions were too large to dissolve by solid state reaction mechanisms. Indeed, the variation in perovskite abundance noted by XRD may in part be explained by different milling efficacy. Future work will use fine $CaTiO_3$ powder as the Ca source.

Figure 5 shows Ce $L_3$ X-ray Absorption Near Edge Structure (XANES) for $Ca_{0.75}Ce_{0.25}ZrTi_{1.625}Fe_{0.375}O_7$ samples fabricated by HIP and by CUP. For comparison, data are also shown for $CeO_2$ and $CePO_4$ (monazite) as standards for $Ce^{4+}$ and $Ce^{3+}$ oxidation states, respectively. The XANES data acquired from the HIP sample (prepared by milling at 4.32 m/s for 30 min with zinc stearate) are representative of data obtained from the entire suite of samples prepared using different lubricants and milling conditions. The Ce $L_3$ edge XANES of $Ce^{3+}$ (e.g., $CePO_4$) is characterized by a white line comprising a single intense feature attributed to the transition from an initial $2p^64f^15d^0$ state to a $2p^54f^15d^1$ final state, modified by local density of unoccupied states (note: the term *white line* refers to strong absorption feature(s) associated with the crest of the X-ray absorption edge). In contrast, the Ce $L_3$ edge XANES of $Ce^{4+}$ (e.g. $CeO_2$) is characterized by a white line comprising two features of lower relative intensity. Following the notation convention employed by Bianconi,[36] the consensus is that these two features, labeled A
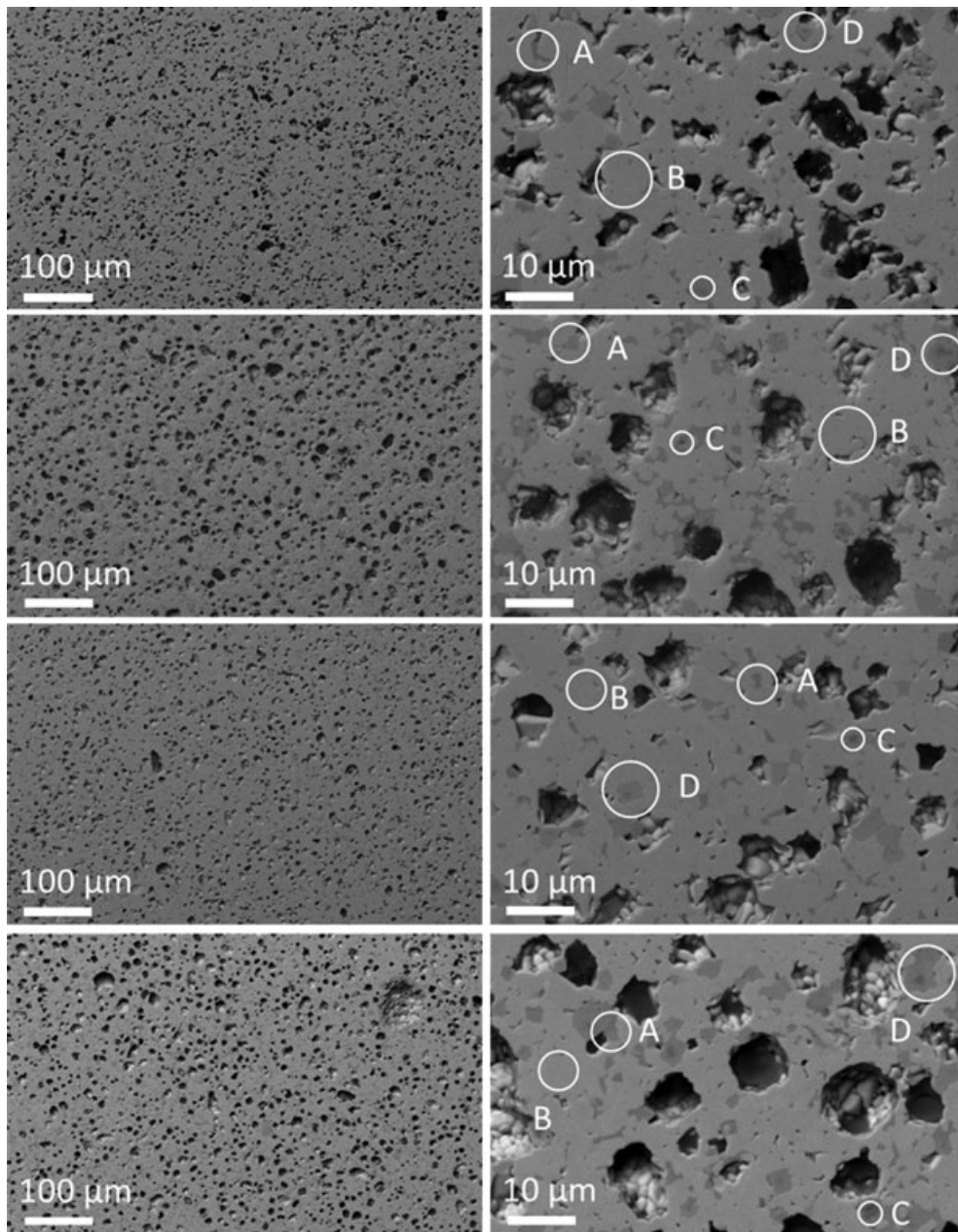
*Fig. 2.   Illustrative SEM images from samples prepared by hot isostatic pressing of powders prepared by attrition milling at 4.32 m/s for 30 minutes with various lubricants. Images on the left are 200× magnification, while right are 1500x. All were taken in the backscattering mode at 15 kV acceleration. From top to bottom samples were prepared with lubricants of zinc sterate, Ceridust$^{TM}$, polyethylene glycol, oleic acid. Phases identified, (A) ilmenite (possibly in solid solution with hematite), (B) zirconolite, (C) perovskite core, (D) perovskite rim. See Figure 3 for EDX spectra.*

and B in Fig. 5, are due to transition from an initial $2p^6 4f^0 5d^0$ state to: (a) the $2p^5 4f^0 5d^1$ final state; and (b) the $2p^5 4f^1 5d^1 \underline{L}^1$ final state (where $L^n$ denotes a ligand hole).[36–40] Other more subtle features are also observed. Feature C is considered to be associated with transition

to a $2p^5 4f^2 5d^1 \underline{L}^2$ final state; whereas, the weak feature D is assigned to quadrupole transitions.[37–40]

The XANES data shown in Fig. 5 permit estimation of the Ce oxidation state in the ceramic products by fitting a linear combination of $CeO_2$ and $CePO_4$ data,
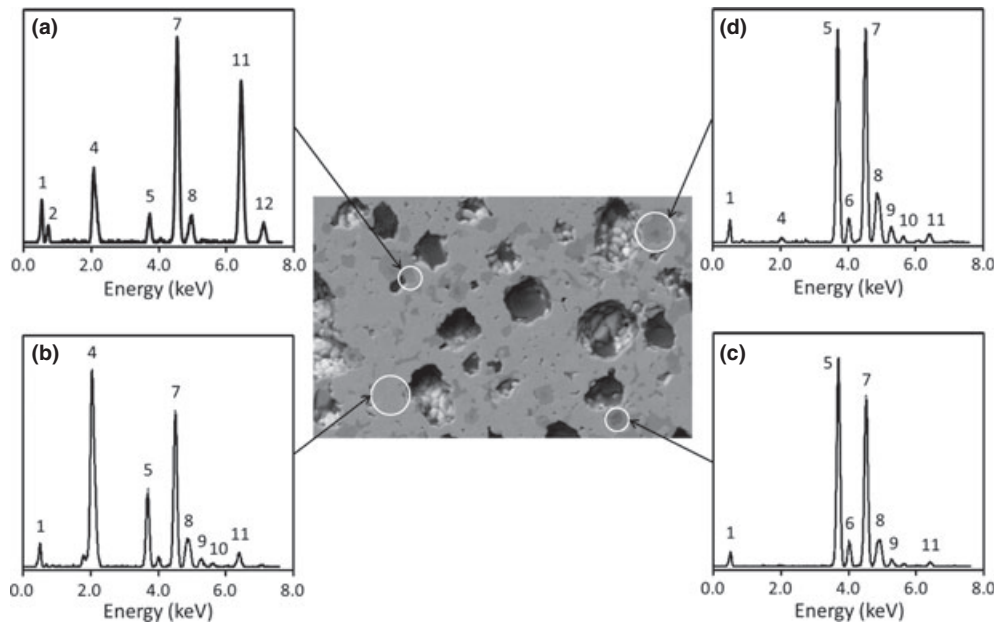
Fig. 3. *EDX spectra for four different grains in microstructure of a sample prepared by hot isostatic pressing of powder prepared by attrition milling at 4.32 m/s for 30 minutes samples with oleic acid as a lubricant. (A) ilmenite (possibly in solid solution with hematite), (B) zirconolite, (C) perovskite core, (D) perovskite rim. See Table 3 for signal identification.*

**Table 3. EDX Signal Assignments for Fig. 3 (*Note: Emission Lines Overlap)**

| Signal | Energy (keV) | Assignment |
|---|---|---|
| 1 | 0.5 | $O(K\alpha)$ |
| 2 | 0.7 | $Fe(L\alpha)$ |
| 3 | 1.8 | $Zr(L\alpha)$ |
| 4 | 2.1 | $Zr(L\alpha)$ |
| 5 | 3.7 | $Ca(K\alpha)$ |
| 6 | 4.0 | $Ca(K\beta)$ |
| 7 | 4.5 | $Ti(K\alpha)$ |
| 8 | 4.7–4.9 | $Ce(L\alpha)/Ti(K\beta)$* |
| 9 | 5.4 | $Ce(L\beta)$ |
| 10 | 6.1 | $Ce(L\gamma)$ |
| 11 | 6.4 | $Fe(K\alpha)$ |
| 12 | 7.1 | $Fe(K\beta)$ |

using the Athena software.[32] Analysis of XANES data demonstrated the Ce speciation in zirconolite products consolidated by HIP to be exclusively $(100 \pm 1\%)$ $Ce^{3+}$. In contrast, Ce was speciated in the product consolidated by CUP as $52 \pm 1\%$ $Ce^{3+}$ and $48 \pm 1\%$ $Ce^{4+}$. From consideration of our measurement resolution (0.1 eV) in comparison with the edge shift associated with $Ce^{3+}$ and $Ce^{4+}$ oxidation states (~1.6 eV), we estimate the detection limit of $Ce^{4+}$ in our measurements to be ~6%.

Figure 6 shows $^{57}Fe$ Mössbauer spectra obtained from $Ca_{0.75}Ce_{0.25}ZrTi_{1.625}Fe_{0.375}O_7$ samples fabricated by HIP and by CUP. The Mössbauer data acquired from the HIP sample (prepared by milling at 4.32 m/s for 30 min with zinc stearate) are representative of data obtained from the entire suite of samples prepared using different lubricants and milling conditions. Previous $^{57}Fe$ Mössbauer analysis of Fe doped zirconolites[41,42] showed that spectra could be fitted using two doublets indicating two distinct Fe coordination environments. This was consistent with substitution of Fe across the distinct Ti cations site in monoclinic zirconolite, which adopt sixfold and fivefold symmetry in a 2:1 ratio. Mössbauer parameters (isomer shift – IS, quadrupole splitting – QS, and relative spectral area) for the HIP and CUP samples are presented in Table 4 along with oxidation state, coordination number and phase assignments for each doublet. Two doublets were fitted to the spectra acquired from the CUP sample, Fig. 6(a); IS and QS of the doublets were consistent with the presence of sixfold and fivefold coordinated $Fe^{3+}$ as previously observed.[41,42] The spectra acquired from the HIP sample, Fig. 6(b), were more complex indicating the presence of contributions in addition to those observed in the CUP sample. Microstructure analysis of the HIP samples (Figs 2–4) indicated that the Fe was predominantly located in the zirconolite and ilmenite minor phase. By comparison
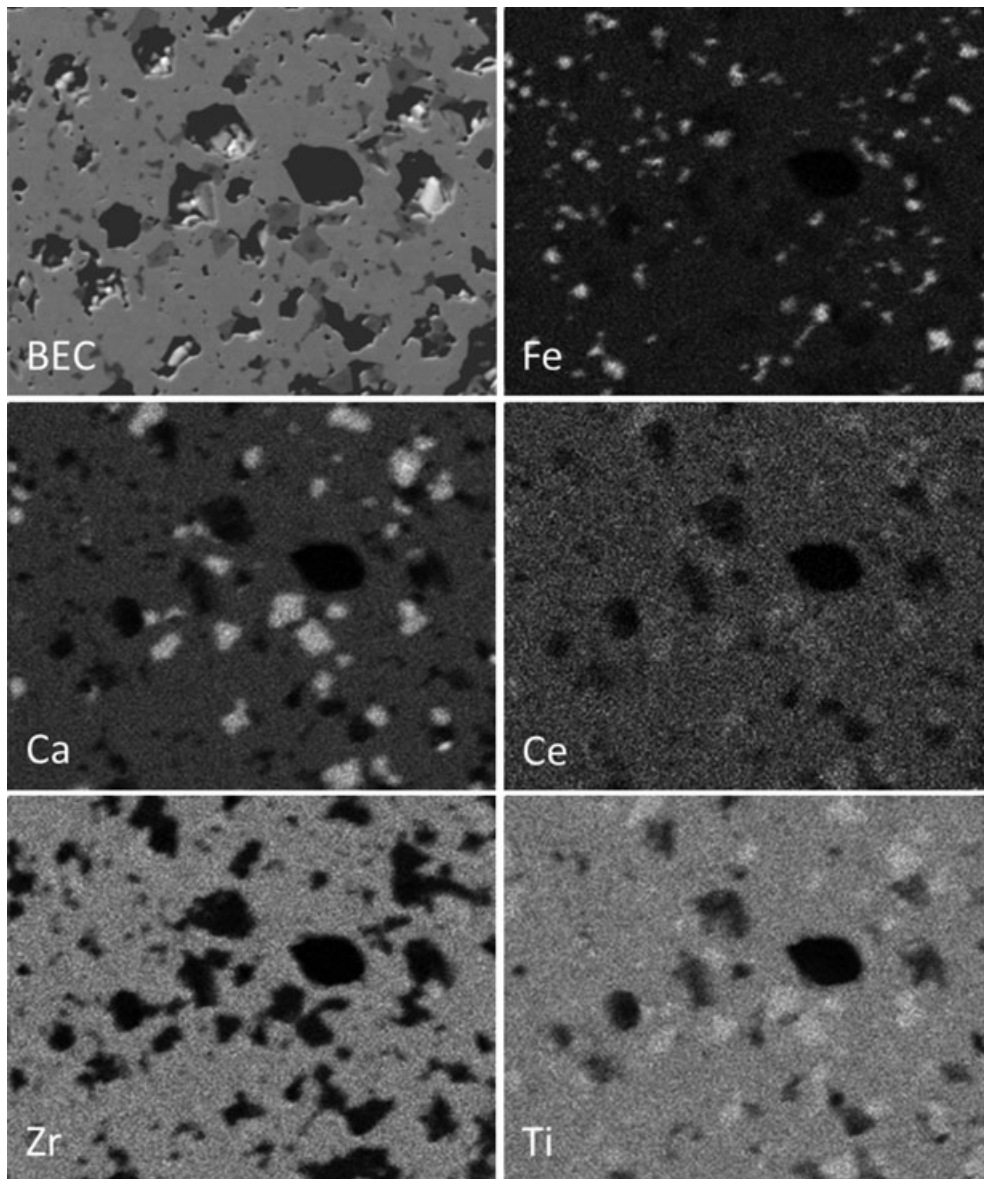
*Fig. 4.   Elemental maps of the microstructure of a sample prepared by hot isostatic pressing of powder prepared by attrition milling at 4.32 m/s for 30 min, with polyethylene glycol as a lubricant. Each image is labeled with its respective element and the backscattered image labeled as 'BEC'.*

with published Mössbauer spectra,[43] the doublet with IS = $1.00 \pm 0.02$ mm/s and QS = $0.59 \pm 0.02$ mm/s was attributed to $Fe^{2+}$ in the ilmenite minor phase. From inspection of the relative spectral areas, the contribution from $Fe^{2+}$ in ilmenite was determined to be $13 \pm 1\%$ of the total Fe inventory. This is consistent with the observed content of ilmenite (ca. 10 %) as estimated from backscattered SEM images (Fig. 2) and elemental maps (Fig. 4). After correcting for the $Fe^{2+}$ contribution from ilmenite, the relative ratio of $Fe^{3+}/Fe^{2+}$ in zircono-lite was calculated to be $85 \pm 1\%$ $Fe^{3+}/15 \pm 1\%$ $Fe^{2+}$ (assuming negligible partitioning of Fe into other phases), consistent with Figs 2–4.

## Discussion

Only three of the selected lubricants succeeded in keeping the powders free flowing during milling. In examining the chemical structure of the lubricants, it is
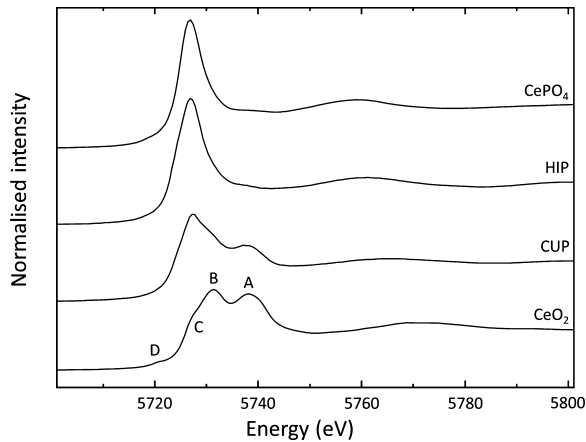
*Fig. 5.  X-ray absorption near edge spectra of HIP and CUP zirconolite samples overlaid with reference compound spectra collected at the Ce $L_3$ absorption edge.*

noted that Ceridust™ is the only material that does not contain a carboxyl or hydroxyl functional group. The lack of molecular polarity and in turn water insolubility may be the origin of the poor performance of Ceridust™ in this application. As the material lacks the functionality to be soluble within the surface moisture layer on the powder particles, there is potentially no mechanism to coat the particles and act as a lubricant. An adsorbed surface layer of water may also be the cause of powder agglomeration. It is widely recognized that damp powders and humid environments are detrimental to free powder flow. Lubricants are used widely with little appreciation of the fundamentals of their performances and this lack of predictability serves to underline the need for detailed quantitative understanding of additives in milling systems.

It is clear that poor performance during lubricant bake out complicates the fabrication of dense zirconolite
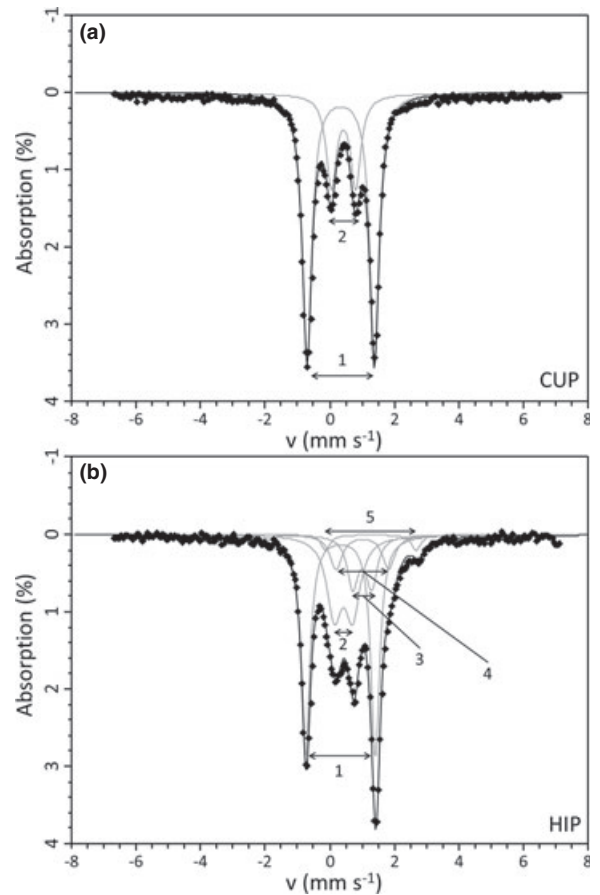


*Fig. 6.  $^{57}Fe$ Mössbauer spectra from HIP and CUP zirconolite samples. Doublets labeled according to assignments in Table 4.*

ceramics by HIP. As described above, the mass loss observed during bake out must be derived from a combination of sources: direct lubricant volatilization, partial lubricant removal by pyrolysis, powder removal, and moisture losses. The removal of any powder is clearly

**Table 4.  Mössbauer Parameters ($\pm$0.02 mm/s) for HIP and CUP Zirconolite Samples with Assignment of Fe Speciation, Coordination Number, and Phase**

| IS (mm/s) | QS (mm/s) | FWHM (mm/s) | Area (%) | Speciation | Coordination Number | Phase |
|---|---|---|---|---|---|---|
| HIP | | | | | | |
| 1  0.36 | 0.57 | 0.27 | 27 | $Fe^{3+}$ | VI | Zirconolite |
| 2  0.29 | 2.17 | 0.16 | 47 | $Fe^{3+}$ | V | Zirconolite |
| 3  1.00 | 0.59 | 0.21 | 13 | $Fe^{2+}$ | VI | ilmenite |
| 4  1.01 | 1.63 | 0.23 | 10 | $Fe^{2+}$ | VI | Zirconolite |
| 5  1.28 | 2.81 | 0.17 | 3 | $Fe^{2+}$ | VI | Zirconolite |
| CUP | | | | | | |
| 1  0.35 | 0.75 | 0.19 | 27 | $Fe^{3+}$ | VI | Zirconolite |
| 2  0.28 | 2.09 | 0.18 | 73 | $Fe^{3+}$ | V | Zirconolite |

unacceptable in a radioactive processing environment and it is possible to prevent powders from being removed by the addition of a sintered metal filter at the base of the evacuation tube. This filter could allow the vaporized lubricant to leave the HIP can without any further powder disturbances. While the HIP can containing the material was heated to 600°C, far above the stated boiling points of the lubricants, the additives were not completely removed in the present study. Consolidation of the powder batch prior to loading into the HIP can, to improve the green packing density and thus the final wasteform density, combined with bake out under vacuum at 600°C, could be expected to result in pyrolysis of the entrained lubricant producing a carbonaceous material.[44] Subsequent high-temperature reaction with the wasteform material under vacuum, within the HIP can, would be expected to produce carbon monoxide (see below). This reasoning would explain the destruction of the ceramic products, through the expansion of internally entrained gas, during high-temperature annealing. This behavior does not give confidence that the wasteform could perform acceptably in an accident (fire) scenario.

The temperature required for lubricant bake out was previously investigated by Chandler *et al.*[45] Thermal analysis showed an increase in the temperature required to fully remove polyethylene glycol (molecular weight 8000) from loose powders and pucks (large pellets) of a candidate wasteform material when compared to polyethylene glycol in isolation from any powder. It was demonstrated that the decomposition region shifted upwards by approximately 75°C. While Chandler *et al.* did not explain this change, it is thought that some combination of reduced heat transfer in the material, leading to lower internal temperatures, and increased diffusional pathway length for the gases through the material, may have increased the overall decomposition temperatures. Repeating these experiments with slower ramp rates, ensuring thermal equilibrium in the powders and pucks is reached at every stage, may prove illuminating.

Consideration and comparison of Ce and Fe speciation in the ceramic products fabricated by HIP and CUP provides further evidence of incomplete removal of lubricants. The target composition was $Ca_{0.75}Ce_{0.25}ZrTi_{1.625}Fe_{0.375}O_7$, with substitution of $Ce^{4+}$ for $Ca^{2+}$ charge balanced by $Fe^{3+}/Fe^{2+}$ on the $Ti^{4+}$ site, in the ratio 66/34%. Ce $L_3$ edge XANES and $^{57}Fe$ Mössbauer data indicate the actual solid solution mechanism to be substitution of $Ce^{3+}$ for $Ca^{2+}$, implying ca. 0.1 oxygen vacancies per formula unit, in order to stabilize the observed $85 \pm 1\%/15 \pm 1\%$ ratio of $Fe^{3+}/Fe^{2+}$. Assuming this reduction to be mediated by reaction of entrained carbon to form carbon monoxide (produced by lubricant pyrolysis as described above), we require 0.1 moles of entrained carbon per mole of product, equivalent to 0.3% carbon by weight. This corresponds to retention of ca. 64% of the pyrolysed lubricant as residual pyrolytic carbon by weight. Under the prescribed process conditions it can be shown that the ceramic product must contain ca. 16 % enclosed porosity in order to accommodate the carbon monoxide produced by the mechanism described above. This is consistent with the average density of the ceramic products, determined to be 85 % of theoretical. Investigation of a ceramic specimen of $Ca_{0.75}Ce_{0.25}ZrTi_{1.625}Fe_{0.375}O_7$ consolidated by CUP and sintered under air provided further insight on the mechanism of charge compensation and lubricant burn out. In this case, the density of the ceramic product was 96 % of theoretical and Ce was determined to be speciated as $Ce^{3+}$ and $Ce^{4+}$, in equal quantity, fully charge compensated by $Fe^{3+}$. In this case, oxidizing conditions in an open furnace enabled complete destruction and removal of the lubricant, leading to a ceramic product with minimal residual open porosity. The absence of reducing agents during the sintering cycle helps to retain $Ce^{4+}$, but it is noted that if all Fe is present as $Fe^{3+}$ then the composition $Ca_{0.75}Ce_{0.25}ZrTi_{1.625}Fe_{0.375}O_7$ requires equal amounts of $Ce^{3+}$ and $Ce^{4+}$, as demonstrated by Ce $L_3$ edge XANES data.

Based on this study, removing the lubricant from milled powders while in the HIP can would appear to be a flawed approach. Increasing the temperature and duration of the removal step is unlikely to increase the proportion of lubricant removed as we have shown that quantitative pyrolysis of the lubricant, leading to entrained carbon, already occurs at the current bake out temperature, which is well above the stated lubricant boiling point (even allowing for the potential boiling point elevation as reported by Chandler *et al.*[45]). It may be possible to remove the lubricants from the milled powders before they are packed into the HIP can. However, working with loose powders in an active environment is often impractical due to the increased dusting and worker dose uptake. Packing material directly into a HIP can from a mill is very attractive in its simplicity. Thus, any organic additive must be easily removed by heating under vacuum or eliminated.

Preliminary work by the authors has shown that by introducing electrical conductivity into the precursor oxides (typically by reducing $Ti^{4+}$ to $Ti^{3+}$ and in doing so forming a semi-conducting Magnéli phase, e.g., $Ti_5O_9$), leads to powders that remain free flowing during milling. It is thought that minimization of tribo-electric charging helps to mitigate powder agglomerations. Through

careful modification of the charge compensation species added to the precursor blend, the $Ti^{3+}$ will be accommodated in the final wasteform, replicating the role of $Fe^{2+/3+}$ here, and eliminating the difficult lubricant removal step. An alternative approach is the use of fumed metal oxides. These materials are nano-crystalline oxides agglomerated into secondary structures to give an extremely low powder density with a very large surface area. They are widely recognized as useful flow promoters with dry powders.[46] The addition of, for example, fumed $Al_2O_3$ has shown promise during preliminary trials by the authors, however difficulties have arisen in respect to temperature control during milling. One further option is a modification of the mill internals. The addition of a method to sweep constantly the base of the mill may prevent an agglomeration of powders ever occurring. This could be by the addition of a trapezoidal bar to the agitator shaft. The bar would sit horizontally at the base of the mill and rotate with the agitator shaft. This bar is shaped so that with each rotation, the bottom layers of milling media, and powders, are lifted into the mill promoting powder circulation and helping to minimize powder compactions. In reality, it is likely that some combination of introduced conductivity, modified lubricant and a modified mill may be required to provide a suitable plutonium wasteform manufacturing line.

## Conclusions

It was thought that there would be a correlation between the aggressiveness of milling and the phase development in the wasteform; the results do not confirm this hypothesis as the inability to fully remove the lubricant has masked any relationship. It can be concluded that zinc stearate, polyethylene glycol and oleic acid are suitable for use as a lubricant in an attrition mill, operated without carrier fluid, with the metal oxides precursor components as they kept the powders free flowing during milling. Ceridust™ has, however, been shown not to be suitable in this application.

The results do not conclusively show how aggressive the milling must be to produce ceramics densities above 92% of theoretical. The failure to remove the lubricant added to aid milling has undermined any attempts to assess wasteform performance. Pyrolysis of entrained lubricant during bake out of the HIP can produced a carbonaceous residue which reduced $Ce^{4+}$ to $Ce^{3+}$ during the processing cycle, producing CO and hence ceramic bodies with considerable interconnected porosity.

While the use of attrition mills warrants further investigation, the specific method outlined in this article is not recommended for implementation in its current form.

## References

1. The Health and Safety Executive, Annual Civil Plutonium and Uranium Figures as of 31st December 2006, 2006. Available at http://www.hse.gov.uk/nuclear/safeguards/civilplut.htm (accessed May 18, 2012).
2. F. von Hippel, R. Ewing, R. Garwin, and A. Macfarlane, *Nature*, 485, 167–168 (2012).
3. Management of the UK's Plutonium Stocks: A consultation response on the long term management of UK-owned separated civil plutonium, URN 11D/819, 1 December 2011.
4. The Nuclear Decommissioning Authority, Plutonium Credible Options Analysis, 2010. Available at http://www.nda.gov.uk/documents/upload/Plutonium-Credible-Options-Analysis-redacted-2010.pdf (accessed May 18, 2012).
5. The Department of Energy and Climate Change, Government Response to Consultation on Management of UK's Plutonium Stocks, 2011. Available at http://www.decc.gov.uk/en/content/cms/consultations/plutonium/plutonium.aspx (accessed May 18, 2012).
6. W. T. Watson, "CSER 96-027: Storage of Cemented Plutonium Residue Containers in 55 Gallon Drums," 1997. Available at http://www.osti.gov/bridge/product.biblio.jsp?osti_id=289278 (accessed May 18, 2012).
7. The Nuclear Decommissioning Authority, The 2010 UK Radioactive Waste Inventory: Main Report, 2010. Available at http://www.nda.gov.uk/ukinventory/documents/Reports/upload/2010-UK-Radioactive-Waste-Inventory-Main-Report.pdf (accessed May 18, 2012).
8. V. V. Kushnikov, Y. I. Matyunin, T. V. Smelova, and A. V. Demin, *Scientific Basis for Nuclear Waste Management XX*, eds., W. J. Gray and I. R. Triay. Materials Research Society Conference Proceedings. Materials Research Society, Warrendale, Vol. 465, 55–64, 1997.
9. W. E. Lee, M. I. Ojovan, M. C. Stennett, and N. C. Hyatt, *Adv. Appl. Ceram.*, 105 [1], 3–12 (2006).
10. J. A. C. Marples, *Vitrification of Plutonium for Disposal*, Vol. 4, 179–195, Kluwer Academic Publ., Dordrecht, 1996.
11. J. M. McCormick and D. B. Bullen, *Policy Studies J.*, 26 [4], 682–702 (1998).
12. E. Trauwaert and M. Demonie, *Plutonium Handling and Vitrification: Main Process Steps and their Cost Evaluation*, Vol. 4, 51–57, Kluwer Academic Publ., Dordrecht, 1996.
13. J. M. McKibben and G. G. Wicks, *Vitrification of Excess Plutonium*, Presented at the International Policy Forum: Management and Disposition of Nuclear Weapons Materials, Leesburg, VA, 1994.
14. I. W. Donald, B. L. Metcalfe, and R. N. J. Taylor, *J. Mater. Sci.*, 32 [22], 5851–5887 (1997).
15. R. C. Ewing, W. J. Weber, and W. Lutze, *Crystalline Ceramics: Waste Forms for the Disposal of Weapons Plutonium*, Vol. 4, 65–83. Kluwer Academic Publ., Dordrecht, 1996.
16. W. L. Gong, W. Lutze, and R. C. Ewing, *J. Nucl. Mater.*, 277 [2–3], 239–249 (2000).

17. M. C. Stennett, N. C. Hyatt, M. Gilbert, F. R. Livens, and E. R. Maddrell, *Scientific Basis for Nuclear Waste Management XXXI*, eds., W. E. Lee, J. W. Roberts, N. C. Hyatt, and R. W. Grimes. Materials Research Society Symposium Proceedings. Materials Research Society, Warrendale, Vol. 1107, 413–420, 2008.

18. S. X. Wang, B. D. Begg, L. M. Wang, R. C. Ewing, W. J. Weber, and K. V. G. Kutty, *J. Mater. Res.*, 14 [12], 4470–4473 (1999).

19. W. J. Weber, *et al.*, *J. Mater. Res.*, 13 [6], 1434–1484 (1998).

20. M. C. Stennett, E. R. Maddrell, C. R. Scales, F. R. Livens, M. Gilbert, and N. C. Hyatt, *Scientific Basis for Nuclear Waste Management XXX*, eds., D. Dunn, C. Poinssot, and B. Begg, Materials Research Society Symposium Proceedings. Materials Research Society, Warrendale, Vol. 985, 145–150, 2007.

21. D. P. Reid, N. C. Hyatt, M. C. Stennett, and E. R. Maddrell, *Materials World*, Vol. 19, 26–28, 2011.

22. H. V. Atkinson and S. Davies, *Metall. Mater. Trans. A*, 31 [12], 2981–3000 (2000).

23. M. H. Bocanegra-Bernal, *J. Mater. Sci.*, 39 [21], 6399–6420 (2004).

24. A. E. Ringwood, S. E. Kesson, N. G. Ware, W. Hibberson, and A. Major, *Nature*, 278 [5701], 219–223 (1979).

25. M. R. Gilbert, *et al.*, *IOP Conference Series: Mat. Sci. Eng.*, 9 [1], 012007 (2010).

26. K. P. Hart, *et al.*, *Scientific Basis for Nuclear Waste Management XXI*, eds. I. G. McKinley and C. McCombie, Materials Research Society Symposium Proceedings. Materials Research Society, Warrendale, Vol. 506, 161–168, 1998.

27. G. R. Lumpkin, *Elements*, 2 [6], 365–372 (2006).

28. Y. Zhang, M. W. A. Stewart, H. Li, M. L. Carter, E. R. Vance, and S. Moricca, *J. Nucl. Mater.*, 395 [1–3], 69–74 (2009).

29. T. Williams, *Nucl. Eng. J.*, 36 [2], 131–135 (1997).

30. P. A. Bingham, R. J. Hand, M. C. Stennett, N. C. Hyatt, and M. T. Harrison, *Scientific Basis for Nuclear Waste Management XXXI*, eds W. E. Lee, J. W. Roberts, N. C. Hyatt, and R. W. Grimes, Materials Research Society Symposium Proceedings. Materials Research Society, Warrendale, Vol. 1107, 421–428, 2008.

31. R. D. Shannon and C. T. Prewitt, *Acta Crystallogr. Sect. B. – Struct. Crystallogr. Crystal Chem.*, B25, 925 (1969).

32. B. Ravel and M. Newville, *J. Synchrotron Radiat.*, 12 [4], 537–541 (2005).

33. D. G. Rancourt and K. Lagarec, "Recoil, Mössbauer Spectral Analysis Software for Windows," 1998. Available at http://www.kfki.hu/~mixhp/doc/pro/recoil.txt (accessed May 10, 2012).

34. H. F. Shaw, "Determination of the Open and Closed Porosity in an Immobilized Pu Ceramic Wasteform. UCRL-ID-132605," 1998. Available at http://e-reports-ext.llnl.gov/pdf/235547.pdf (accessed May 18, 2012).

35. C. J. Howard, G. R. Lumpkin, R. I. Smith, and Z. Zhang, *J. Solid State Chem.*, 177 [8], 2726–2732 (2004).

36. A. Bianconi, *et al.*, *Phys. Rev.*, B35, 806–812 (1987).

37. A. Soldatov, T. Ivanchenko, S. Dellalonga, A. Kotani, Y. Iwamoto, and A. Bianconi, *Phys. Rev.*, B50, 5074–5080 (1994).

38. M. C. Stennett, C. L. Freeman, A. S. Gandy, and N. C. Hyatt, *J. Solid State Chem.*, 192, 172–178 (2012).

39. D. P. Reid, M. C. Stennett, and N. C. Hyatt, *J. Solid State Chem.*, 191, 2–9 (2012).

40. M. C. Stennett, C. L. Corkhill, L. A. Marshall, and N. C. Hyatt, *J. Nucl. Mater.*, 432, 182–188 (2013).

41. F. J. Berry, G. R. Lumpkin, G. Oates, and K. R. Whittle, *Hyperfine Interact.*, 166, 363–366 (2005).

42. S. D. Forder, P. A. Bingham, O. J. McGann, M. C. Stennett, and N. C. Hyatt, *Hyperfine Interact.*, 217, 83–90 (2013).

43. W. Kim, S. J. Moon, and C. S. Kim, *Hyperfine Interact.*, 185, 167–171 (2008).

44. S. C. Moldoveanu, Ed. "Analytical Pyrolysis of Synthetic Organic Polymers", Techniques and instrumentation in Analytical Chemistry – Vol. 25, 2005.

45. G. Chandler, A. Cozzi, C. Herman, J. Marra, J. Mitchell, and R. Pierce, Plutonium Immobilization Project Binder Burnout and Sintering Studies (Milestone 6.6a). WSRC-TR-99-00321, 1999. Available at http://www.osti.gov/energycitations/servlets/purl/14277-X5OibI/webviewable/14277.pdf (accessed May 18, 2012).

46. N. Harnby, *Powders and Solids: Developments in Handling and Processing Technologies*, eds., W. Hoyle. Royal Soceity of Chemistry, UMIST, Manchester, 82–92, 2000.